PNAS
www.pnas.org

Supplementary Information for

Unveiling dimensions of stability in complex ecological networks

Virginia Domínguez-García, Vasilis Dakos and Sonia Kéfi

Virginia Dominguez-García
E-mail: virginia@onsager.ugr.com

This PDF file includes:

www.pnas.org/cgi/doi/10.1073/pnas.1904470116

Supporting Information Text

1. Change of pairwise correlations with community size

To study if the size of the multispecies trophic communities (i.e. species richness) has an effect on how different metrics of stability correlate with each other, we follow the pairwise correlations between all metrics for different community sizes. For each community, we calculate all stability metrics presented in Table 1 in the main text, and study the correlations as a function of community size as follows. For each community size, we sample 100 trophic communities (i.e 100 communities with 5 species, for example) and compute the pairwise correlations among all stability metrics using Spearman's correlation rank, ρ. We repeat this for all community sizes ranging from 5 to 100, and obtain the correlation between metrics as a function of community size.

We then go on to check if those correlations are affected by community size. To do that we are going to compare the value of the correlation rank ρ in three different size scenarios: small communities (composed by 5 to 10 species), medium sized communities (composed by 45 to 55 species) and large communities (with 85 to 95 species). For each size scenario we obtain the average value of the pairwise correlations by averaging over the values of the correlation rank obtained for the sizes within the size range. We consider that pairwise correlations remain unchanged throughout a gradient of species richness if the variation in the average value of the pairwise correlation between the initial and final size scenarios ($\Delta\rho$) is below 0.1. With that, we create three different categories: correlations that keep changing throughout all sizes (~6%, Fig. S1i A-C), correlations that change only in small to medium-sized communities (~50%, Fig. S1i D-F) and correlations that remain constant irrespective of community size (~44%, Fig. S1i G).

From all the correlations that change with size, we identify how many pairwise correlations increase in strength with increasing community size (~21%, Fig. S1i B and E) and how many decrease in strength when the size of the community increases (~32%, Fig. S1i C and F). A small proportion of the correlations changes sign with network size (only ~6%, Fig. S1i A and D).

We represent the effect of community size on correlations in Fig. S1i (a centered rolling mean of 6 was used to plot the lines in this figure in order to reduce the noise and improve the interpretation). To better visualize the behaviour of all pairwise correlations, a matrix-like representation is included in Fig. S1ii. The matrix elements are colored according to which one of the 7 behaviours (A to G) each pairwise correlation belongs to:

A. Correlation strength keeps changing with community size, and it also changes sign. Colored in purple in Fig. S1ii

B. Correlation strength increases with community size. Colored in red in Fig. S1ii

C. Correlation strength decreases with community size. Colored in blue in Fig. S1ii

D. Correlation strength is constant in species-rich communities (>50 species) but changes sign in smaller communities. Colored in light purple in Fig. S1ii

E. Correlation strength increases with community size in communities with less than 50 species and remains constant in species-rich communities. Colored in light red in Fig. S1ii

F. Correlation strength decreases with community size in communities with less than 50 species and remains constant in species-rich communities. Colored in light blue in Fig. S1ii

G. Correlation strength is constant throughout all sizes. Colored in grey in Fig. S1ii

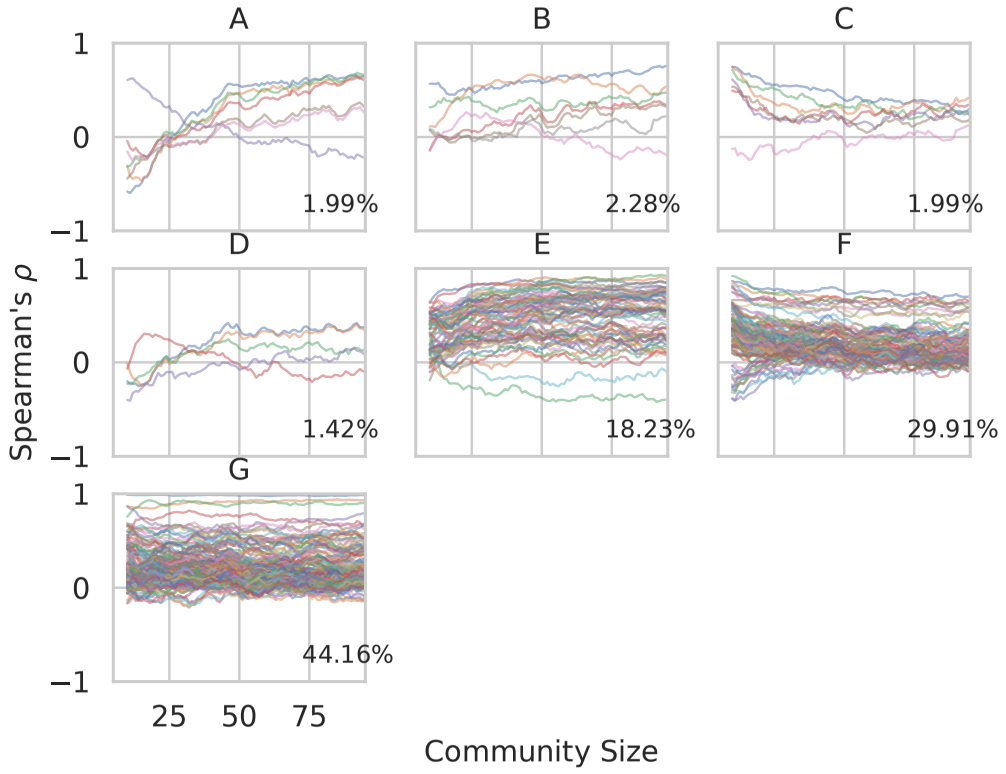

(i) Variations in pairwise Spearman's ρ correlation between all pairs of metrics as a function of community size.

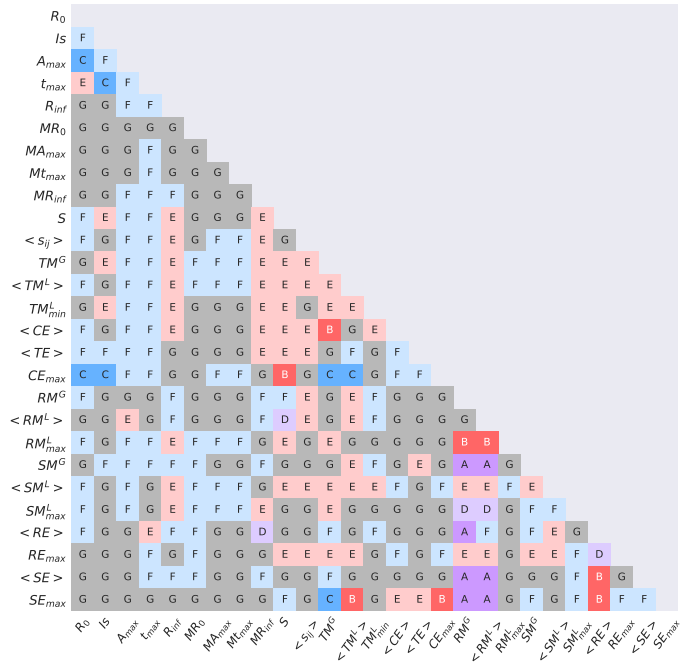

(ii) Visualization of the way pairwise correlations change with network size according to the seven categories presented in the different panels of Fig. S1i.

Fig. S1. Changes in pairwise correlation with network size. **i)** First row (A-C): Pairwise correlations that vary with size throughout all the sizes covered in this study. A) Pairwise correlations that change sign, B) Pairwise correlations that continuously *increase* in strength with community size, C) Pairwise correlations that continuously decrease in strength with community size. Second row (D-F): Pairwise correlations that vary with size only in small to medium-sized communities (i.e. below 50 species) but remain constant for larger communities. We identify three different behaviours: D) pairwise correlations that change sign, E) pairwise correlations that *increase* in strength with community size, F) pairwise correlations that decrease in strength with increasing community size. Third row (G): Pairwise correlations that remain constant throughout all community sizes. In each panel, the digit in the lower right part is the percentage of pairwise correlations (our of a total of 351) that belong to a given category. All pairwise correlations are assigned to one of the seven categories: A to G (see SI Appendix, section 1). **ii)** Classification of all 351 pairs of correlations according to one of the seven behaviours shown in Fig. S1i. Metric names are indicated on the left and lower side of the matrix (see Table 1 in the main text of the paper for their definitions). For each pair of metrics, the letter (and color to help the eye) represents one of the different behaviours, A to G, displayed in the panels of Fig. S1i.

2. Impact of community size on the structure of the stability metrics network

One of the features of complex networks is that the interactions they represent can be structured, e.g. by forming groups of densely connected vertices. We use a community detection method based on maximizing the modularity (hereafter referred to as the 'modularity algorithm', see Materials and Methods), to find groups of densely connected metrics in the stability metrics network.

Because network size has an impact in how different metrics correlate with each other (see section 1 above and "Community size and stability metrics' correlations" in Results), we also study how it affects the structure of the stability network by following the sorting of nodes into different groups along a gradient of community sizes as follows. We start by building the stability metric network for communities composed of 5 to 10 species (see Materials and Methods). We then identify the different groups of metrics using the modularity algorithm and register the identity of the group each node is assigned to. We repeat this procedure for communities of increasing species richness (i.e. network size): 10 to 20 species, 20 to 30 species ,... until a total richness of 90 to 100 species. Since the modularity maximization algorithm is stochastic, for each size, we build 20 stability networks, run the modularity algorithm 10 times for each of them and register the number of times each node is assigned to each group.

We identify three main groups: The 'Early response to pulse' group, (**light green** in Fig. 2A in the main text and Fig. S3) contains measures of the initial and short-term deviations of a community from its reference state after a pulse perturbation. The 'Sensitivities to press' group (**green** in Fig. 2A in the main text and Fig. S3) includes metrics that quantify changes in total and individual species' biomass between post- and pre-perturbed communities after a press perturbation. The 'Distance to threshold' group (**blue** in Fig. 2A in the main text and S3) consists of metrics that measure how easily a system crosses thresholds to new dynamical states, for example the amount of external pressure before a community experiences an abrupt change, the closeness of the rarest species to extinction, the population variability, and secondary extinctions caused by random extinctions.

By looking at the sorting of nodes into the groups found by the modularity algorithm, we find that the only changes involve a small group of metrics: three metrics of initial and transient responses of the most abundant species to pulse perturbations, namely reactivity (R_0), maximum amplification (A_{max}), and time to maximum amplification (t_{max}). These are the only metrics whose group attribution changes with community size (see Table S1). While in communities of less than 20 species, they are found in the same group as the 'Distance to threshold' metrics (blue), they grow progressively disconnected from this group of metrics as community size increases. Reactivity (R_0) disconnects from this group in communities larger than 20 species, and is placed either in the 'Sensitivities to press' (darker green) or in the 'Early response to pulse' (light green). Maximum amplitude (A_{max}) is disconnected from the blue group in communities with a species richness of above 30 species, and it is placed either in the 'Sensitivities to press' (darker green) or in the 'Early response to pulse' groups (light green). Finally, time to maximum amplification (t_{max}) is disconnected from the blue group in communities with more than 70 species, and is placed either in the 'Sensitivities to press' (darker green) or in the 'Early response to pulse' group (light green). Table S1 shows detailed information about how the three metrics are sorted into the different groups as community richness increases. For each size category, the proportion of times each of the metrics was assigned to each group was recorded. Since there is no consistent classification of these three metrics in a group independent of network size, we kept them apart from the other metrics (in grey in Fig. 2A in the main text and in Fig. S3). Note that the three metrics don't form their own group in the sense that the reason they are put together is solely because of their lack of clear group attribution (and not because they are more correlated with each other than with the other metrics).

This study shows that as communities grow more complex (in term of species number), these three metrics, that are driven by the behaviour of the more abundant species (1), are increasingly disconnected from the other metrics. This has implications for quantifying the overall stability of the system: if one is interested in the individual response of species a short time after the disturbance in communities with moderate richness and above (20 species or more), it will be necessary to actually quantify these individual behaviours specifically, as they are not well represented by any of the other metrics.

Table S1. Group assignment according to the modularity algorithm for the three metrics R_0, A_{max}, and t_{max} as a function of community size

Community size	5-10			10-20			20-30			30-40			40-50		
Metric/Group	E*	D*	S*	E	D	S	E	D	S	E	D	S	E	D	S
R_0	.	1	.	.	1	.	0.05	0.13	0.82	0.27	.	0.73	0.28	.	0.72
A_{max}	.	1	.	.	1	.	0.05	0.77	0.28	0.27	.	0.73	0.28	0.06	0.66
t_{max}	.	1	.	.	1	.	.	1	.	.	1	.	0.06	0.94	.
Community size	50-60			60-70			70-80			80-90			90-100		
Metric/Group	E	D	S	E	D	S	E	D	S	E	D	S	E	D	S
R_0	0.52	.	0.48	0.05	.	0.95	0.04	.	0.96	0.12	.	0.88	0.87	0.04	0.09
A_{max}	0.52	.	0.48	0.05	.	0.95	0.04	.	0.96	0.12	.	0.88	0.74	0.17	0.09
t_{max}	0.40	0.60	.	0.05	0.65	0.30	0.04	0.20	0.76	0.12	0.40	0.48	0.91	.	0.09

* The acronyms for stability groups are E for 'Early response to pulse' (in light green), D for 'Distance to threshold' (in blue) and S for 'Sensitivities to press' (in darker green).

3. Inter and intra-group correlations in the network of stability metrics

The partition of the network provided by the modularity algorithm is formed by groups of metrics that are intensely correlated with other metrics inside the same group and weakly correlated with metrics outside the group. In our framework, that can be understood as the metrics inside a group being largely independent from the metrics outside the group, but being largely redundant with metrics within the same group.

To check to what extent this is indeed the case, we computed the inter and intra-group average correlations. The intra-group average correlation is quantified as the average pairwise correlation between all the metrics inside a group. The inter-group average correlation is the average pairwise correlation between metrics that belong to two different groups. It is possible to visualize both at the same time with a lumped representation of the network of stability metrics (Fig. S2), where each node represents one of the different stability metrics group, and the links the average pairwise correlation between metrics belonging to different groups.

Different partitions of the network generate different lumped networks, and hence different inter and intra-group correlations. We compare two different partitions: the most frequently proposed by the modularity algorithm, in which the three metrics discussed in the previous section (R_0, A_{max}, t_{max}) are assigned to the different three groups according to Table S1 (Fig. S2A), and one where these three metrics are considered separately and placed in an different set (Fig. S2B). In both cases the average inter-group correlation (~0.13) is much weaker than the strength of the correlation between metrics in the same group, validating our hypothesis that these partitions represent groups of relatively independent metrics. Comparing both partitions (Fig. S2 A and B), we see that placing the three discussed metrics aside increases the intra-correlation of the three groups defined by the modularity algorithm ('Early response to pulse' in light green, 'Distance to threshold' in blue and 'Sensitivities to press' in green in Fig. S2) while not having a major impact on the average inter-correlation strengths. In light of this, we decide to use the second partition (Fig. S2B) for our future analyses, and we neither assign the three discussed metrics to any of the three groups, nor to their own independent group (since their intra-group correlation is relatively low in medium-sized and large communities).

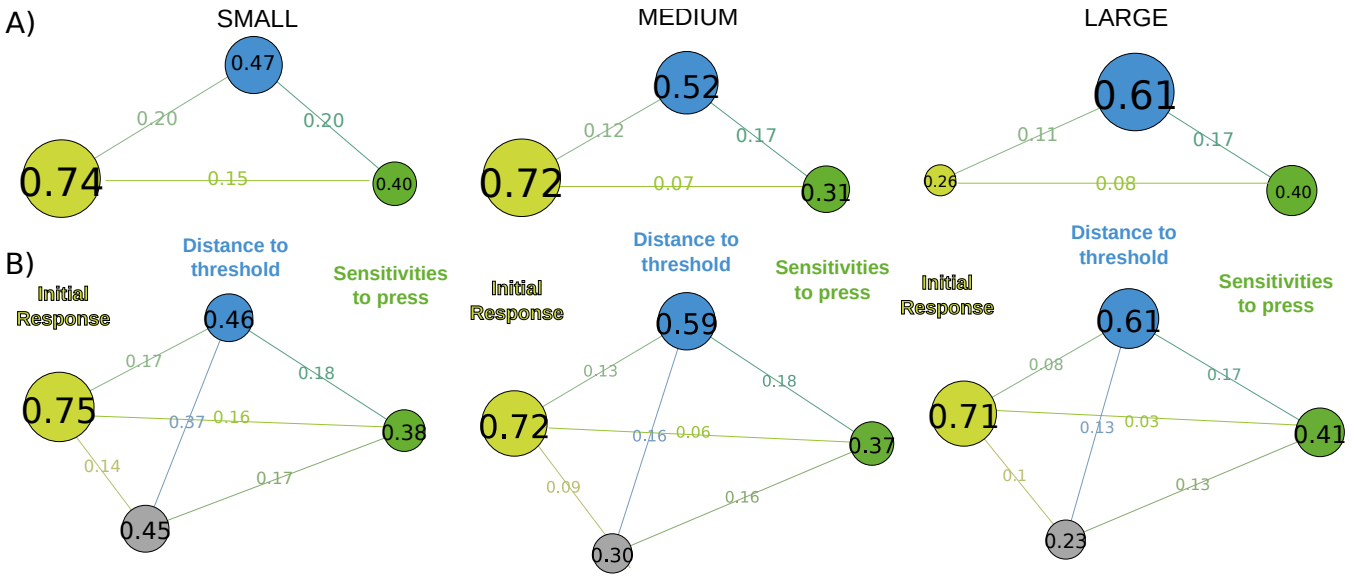

Fig. S2. Intra- and inter-group correlations: Network of correlations between groups, where each node represents one of the different groups identified by the modularity algorithm : 'Early response to pulse' (light green), 'Distance to threshold' (blue), 'Sensitivities to press' (darker green). The grey node represents the three metrics, which were not clearly attributed to one of the three other groups. The size of the nodes is proportional to the intra-group correlation (also shown with the value inside each node). The numbers over the links represent the average correlation between metrics belonging to the two groups connected by that link (inter-group correlation). A) Inter and intra-group correlations considering the most frequent groups obtained from the modularity algorithm. In this case the three grey metrics change from being in the 'Distance to threshold' group (blue) in small communities, to being placed in the 'Sensitivities to press' (darker green) and in the 'Distance to threshold' (blue) groups in medium-size networks, to the 'Early response to pulse' group (light green) in large networks (see Table S1 in main text). B) Inter and intra-group correlations considering the three grey metrics (R_0, A_{max}, and t_{max}) apart from the others.

4. Quantifying stability metrics' (dis)similarity

The modularity algorithm provides a global description of how metrics can be organized in groups of relatively independent stability components, but it does not provide detailed information about the degree of (dis)similarity between different metrics. To examine this, we perform a hierarchical clustering analysis (2, 3). This approach is based on aggregating nodes according to their pairwise correlations (see Materials and Methods). The correlations are used to compute a distance d, equal to 1-ρ, (where ρ is Spearman's rank correlation) between all pairs of metrics. This distance is represented by means of a dendrogram in Fig. 2B in the main text and Fig. S3. The key to interpreting such a dendrogram is to focus on the first 'branch' at which any two metrics are joined together; the further away two metrics are from this 'common ancestor' the less similar they are.

The dendrograms obtained (Fig. S3) are clearly in good agreement with the groups identified by the modularity algorithm, except for the 'resistance to extinction' metric ($< RE >$), represented with a stripped pattern in Fig. 2B in the main text and in Figs. S3ii and S3iii, which is not placed in the same group by both approaches in medium-sized and in large communities. This metric quantifies the average change in total biomass before and after a random extinction, without taking into account the identity of the targeted species. However, the nature of the targeted species has a major influence on the resulting change in total biomass: e.g. deleting an apex predator will generally result in small changes in biomass, while deleting a plant or low-level predator could cause major changes. It is probably because it averages the response across all species in the community that its correlations to other related metrics (e.g. RE_{max}) are weaker and that it casts itself as an outlier. This could mean that it is important to take into account the identity of the targeted species in order to consistently evaluate the effect of extinctions in the total biomass of the community. As a result of the discrepancy between the two methods we applied to place $< RE >$ inside a group, we did not include this metric in the subsequent analyses.

The dendrograms allow to visualize a more detailed structure, with subgroups of similar metrics within the three groups identified by the modularity algorithm. In medium-sized communities, for example, the 'cascading extinctions' ($< CE >$), and 'tolerance to extinction' ($< TE >$) metrics – which measure responses to random extinctions (see Table 1 in main text, or SI section 10 for a full description) – are in the same group (in blue) as 'tolerances to mortality' metrics (mortality increases both at a global (TM^G) and local (TM^L_{min}, $< TM^L >$) scale). Yet, these two responses to extinction are more similar to each other than to any other metric in the same group. As another example, each of the metrics of 'resistance to mortality' (RM^G), 'sensitivity to mortality' (SM^G) and 'tolerance to mortality' (TM^G), that are derived from global attacks (simultaneous increase of the mortality of all species) are always close to their average over local attacks (increase in the mortality of one species): $< RM^L >$, $< SM^L >$ and $< TM^L >$ respectively. This similarity can be interpreted as a "superposition principle" (4), where the global attack is just the sum of the attacks to independent species, and no added amplification emerges when all species are attacked at the same time.

The dendrograms also reveal connections that may not have been apparent based on the modularity algorithm. A clear example in medium-sized communities is the subset inside the blue group (Fig. S3ii or Fig. 2B in main text) composed of five strongly connected metrics of very different nature: 'resilience' (R_{inf}), which is a metric of dynamical stability, 'tolerance to mortality' metrics (TM^G, TM^L_{min}), which assesses structural stability , and 'sensitivity metrics' (S, $< s_{ij} >$), which are based on the inverse Jacobian. This tightly connected subset is also present in large communities, where the it also includes 'cascading extinctions' ($< CE >$). The strong connection that we find between 'resilience' (R_{inf}) and 'tolerance to mortality' metrics (TM^G, TM^L_{min}) can be intuitively understood by noting that they represent different ways of estimating the distance to a dynamical threshold, either by directly testing for the intensity of the stress that leads to the first extinction (5, 6) – our definition of 'tolerance' (see Table 1 in the main text) – or indirectly by means of critical slowing down indicators such as 'resilience' and 'invariability' (7). Also, some of these connections have been previously reported in the literature, such as the relationship between 'resilience' and 'sensitivity' in donor-dependent systems (8), but not much is known about the others (but see (9)), and we still lack a complete theoretical map between most metric relationships.

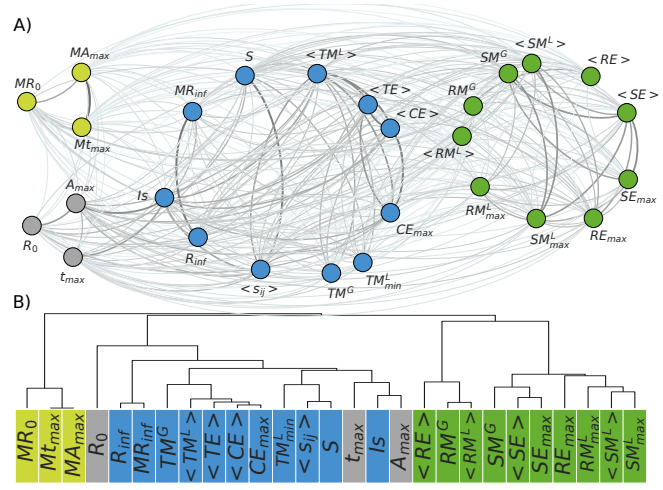

(i) Small communities (5 to 15 species)

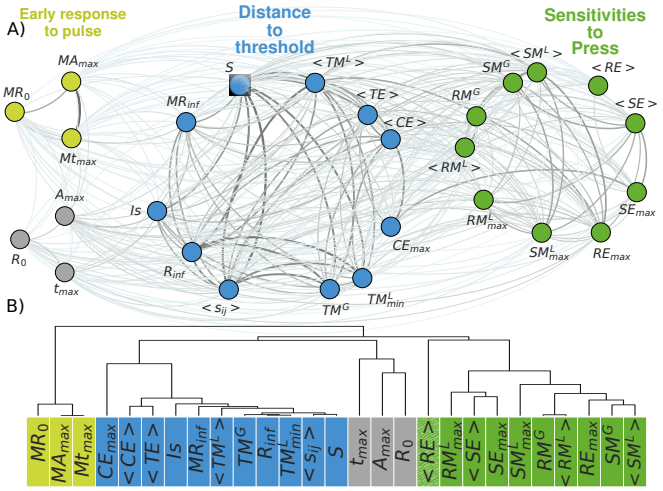

(ii) Medium communities (45 to 55 species)

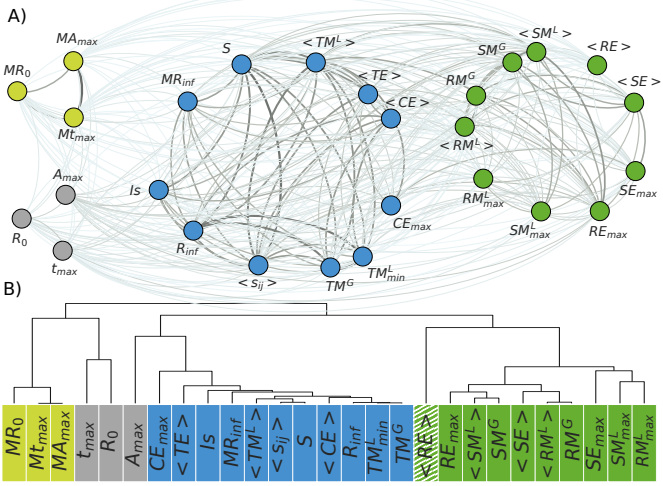

(iii) Large communities (85 to 95 species)

Fig. S3. Analysis of the stability network for communities with different species richness: i) small communities, ii) medium-sized communities and iii) large communities. Upper part of the three panels (A): Networks of stability metrics. Nodes represent the different stability metrics and weighted links the pairwise Spearman's correlation coefficients. Thicker links represent stronger pairwise correlations. The colour of the nodes represents the different groups they are assigned to by the modularity algorithm, with modularity values of i) 0.114, ii) 0.147 and iii) 0.191. We identify them as follows: *Early response to pulse* group in **light green**, the *Distance to threshold* group in **blue** and the *Sensitivities to press* group in **darker green**. In grey are the nodes that the algorithm was not able to unambiguously place in any of the three groups. Lower part of the three panels (B): Dendrogram obtained with the hierarchical clustering analysis on the same network of stability metrics. The dendrograms represent the distances between pairs of metrics. The Cophenet Coefficient correlation, which defines how well the dendrogram distances represent the distances of the original data are: i) 0.87, ii) 0.85 and iii) 0.87).

5. Signs of the correlations among stability metrics

The sign of the correlations does not play a role in defining whether two metrics are providing similar information or not, which is why we have not considered the sign of the correlations until now. However, it becomes important if we want to identify the existence of trade-offs between stability metrics. The existence of a negative correlation would mean that it is not possible to quantify the overall stability of a system in an unequivocal way, since being more stable according to a given stability metric would mean that that community is automatically less stable according to another metric.

However, we found that most pairwise correlations in our trophic communities are positive (meaning that the average value of ρ in each size range is above 0), from ~86% of al 351 correlation pairs in small communities to ~93% in large communities (see Fig. S4 i,ii,iii, and iv). This vast majority of positive correlations is in line with recent experimental findings where multiple positive correlations between stability metrics were found in communities of similar size to our simulated communities (10, 11). Some attention must be paid to small-sized communities, for which a few negative correlations are found.

A. Negative correlations. In small communities the strongest negative correlations take place between 'resistance to mortality' (total change of community biomass after an increase in mortality at the global (RM^G) and at the local -species- scale ($< RM^L >$) and 'resistance to mortality' and 'sensitivity to mortality' (total change in species' biomass after an increase in mortality at the global scale (SM^G)) with a Spearman's rank coefficient of $\rho \sim -0.54$ and $\rho \sim -0.39$ respectively (See Fig. S4 i and iv). This relationship means that larger changes in species populations after a mortality increase are accompanied by smaller changes in total aggregated biomass (i.e the population changes take place in such a way that total change in aggregate biomass is minimised when the species' population experiments larger changes). This compensatory behaviour quickly disappears as richness increases, and we find that in communities with 20 species or more, larger (resp. smaller) changes in species' biomass are reflected in larger (resp. smaller) changes in total biomass. The changes in populations' biomass do not compensate among different species anymore: the majority of species exhibit a change in biomass of the same sign (i.e all increase or all decrease in biomass) and that is reflected in the change of total aggregated biomass of the community being correlated with the changes in the average populations' biomass. That does not mean that there are not any compensation at all (i.e. some species increasing in population while others decrease) but is not enough to have an impact in the average behaviour any more.

As for the rest of negative correlations in small communities, they include the 'resistance to random extinctions' metric ($< RE >$) that measures the average total change of community biomass before and after random extinctions, which we previously classified as an outlier (see SI Appendix, section 4 and Fig. S3), and hence we don't further study its behaviour.

The only important negative correlation (i.e. ρ above 0.3) that remains when the size of the community increases over 20 species is between R_0 and t_{max} (i.e. reactivity and time to maximum amplification), as we can see in Fig. S4 ii, iii, and iv. While the relationship between these two metrics has been studied previously and found to be complex (12), our results hint that communities with abundant species that initially deviate fast (i.e. high R_0) also start to recover early (i.e. low t_{max}), while communities with less reactive abundant species tend to take longer before they start their recovery.

B. Abundance of positive correlations. As we mentioned before, the dominance of positive correlations is in agreement with recent experimental findings, where multiple positive correlations between different stability metrics were found in communities of similar sizes (10, 11) (only invasions seemed to be negatively correlated to other metrics of stability (11)). The metrics used here may not be entirely identical to those used in these experimental studies, nonetheless there are clear similarities. For example, we find a correlation (ρ =0.37) in small communities between population invariability (I_s) and a measure of resistance (SM^G) that is similar to the one used by (11), and also between invariability (I_s) and the number of secondary extinctions ($< CE >$) (ρ =0.57), and between the number of secondary extinctions ($< CE >$) and sensitivity measured as (SM^G) (ρ =0.31). We also find a correlation between invariability (Is) and sensitivity to small press perturbations – i.e. without extinctions – (S) in small communities (ρ =0.54) in agreement with (10).

It is worth noting that in light of these results, some communities will be able to respond better than others to *any* of the tested disturbances. Conversely, some communities will be globally weaker than others to all tested perturbations. For example, less 'resilient' communities (low R_{inf}), where some of the rare species are closer to extinction, will also be able to accommodate a smaller amount of stress before a major shift happens in the form of the loss of one or more species in the community (i.e they have a smaller 'tolerances to mortality increase' (lower TM^G, TM^L_{min}, and $< TM^L >$). Also they tend to show a higher number of 'cascading extinctions' ($< CE >$) and a smaller 'tolerance to random extinctions' ($< TE >$), meaning that the community will collapse after a few species are lost. This, however, can also work in the opposite way: communities that already have difficulties withstanding a given stress according to a given stability metric, will probably be more vulnerable to other stresses as well.

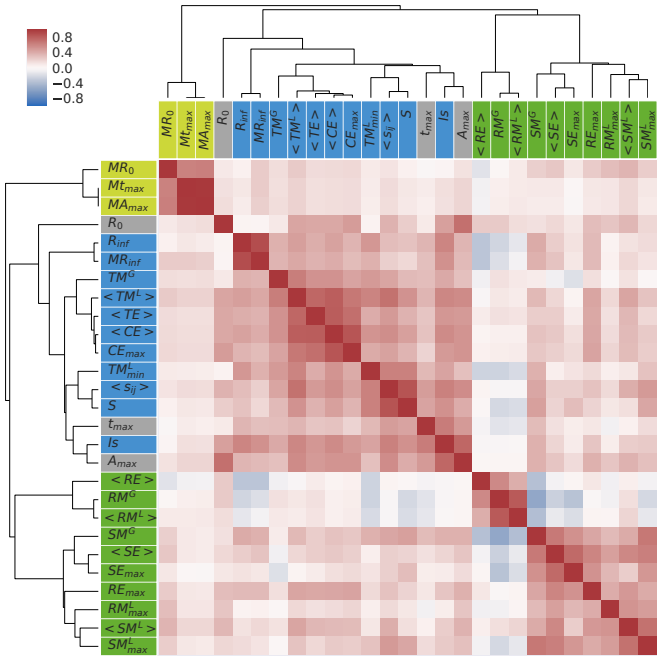

(i) Small communities (5 to 15 species)

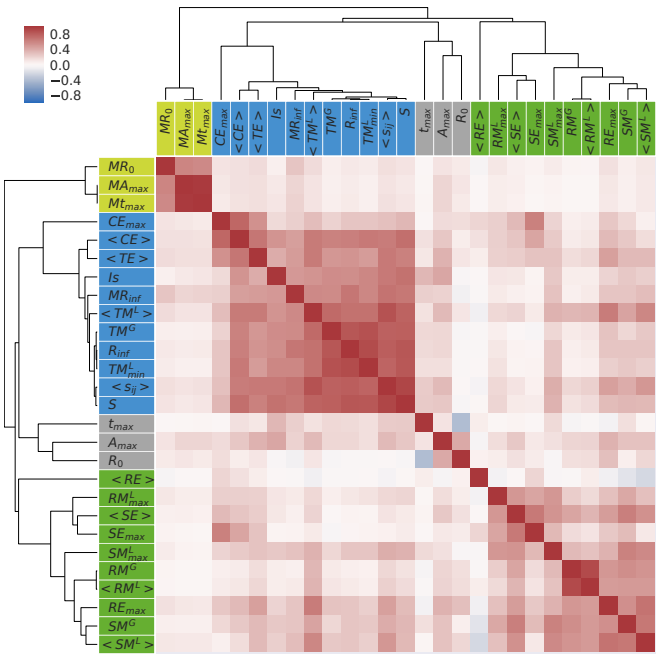

(ii) Medium communities (45 to 55 species)

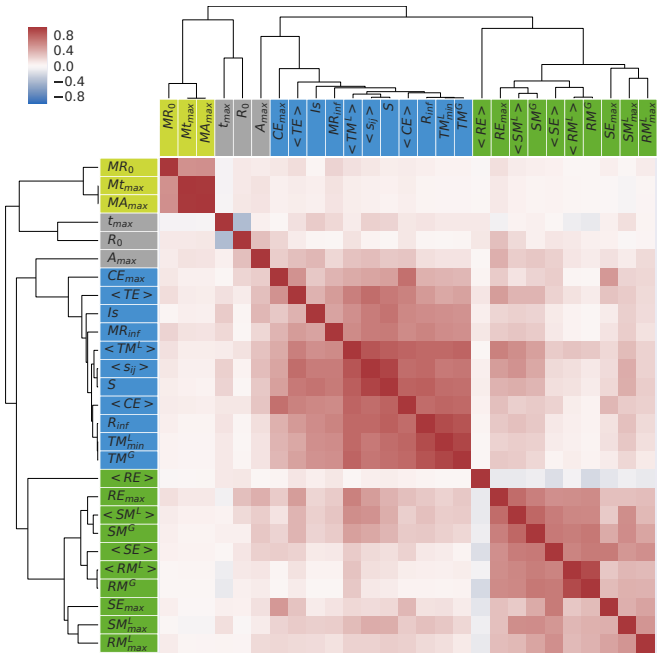

(iii) Large communities (85 to 95 species)

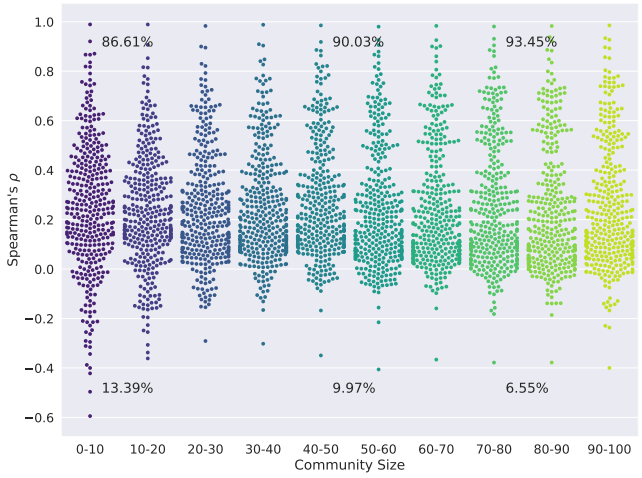

(iv) Violin plot of pairwise correlation between metrics.

Fig. S4. i, ii and iii: Signed stability network, here shown as a correlation matrix heat-map, for communities with different species richness. The rows and columns of the matrix are the different metrics considered in the study, and each matrix element is the signed correlation between that pair of metrics. This value is represented by a color code (included in the legend) as follows: the sign of the correlation is shown in different colors: Positive correlations are showed in red while negative correlations are showed in blue; the intensity of the color is proportional to the intensity of the correlation. As we can see, in all cases most metrics share a positive correlation (or are independent). iv: Violin plot of all the pairwise correlations among metrics as a function of community size. The first size category contains pairwise correlations in communities with richness between 0 and 10 species, the second between 10 and 20 species, the third between 20 and 30 and so on. As size increases most of the pairwise correlations become positive, but some anti-correlated metrics remain (although it is a weak relationship). The two stronger negative correlations are between R_0 and t_{max} (-0.4) and between $< RE >$ and $< SE >$ (-0.2). The percentages in the upper/lower part of the graphic indicate the proportion of positive/negative correlations in small, medium sized and large communities.

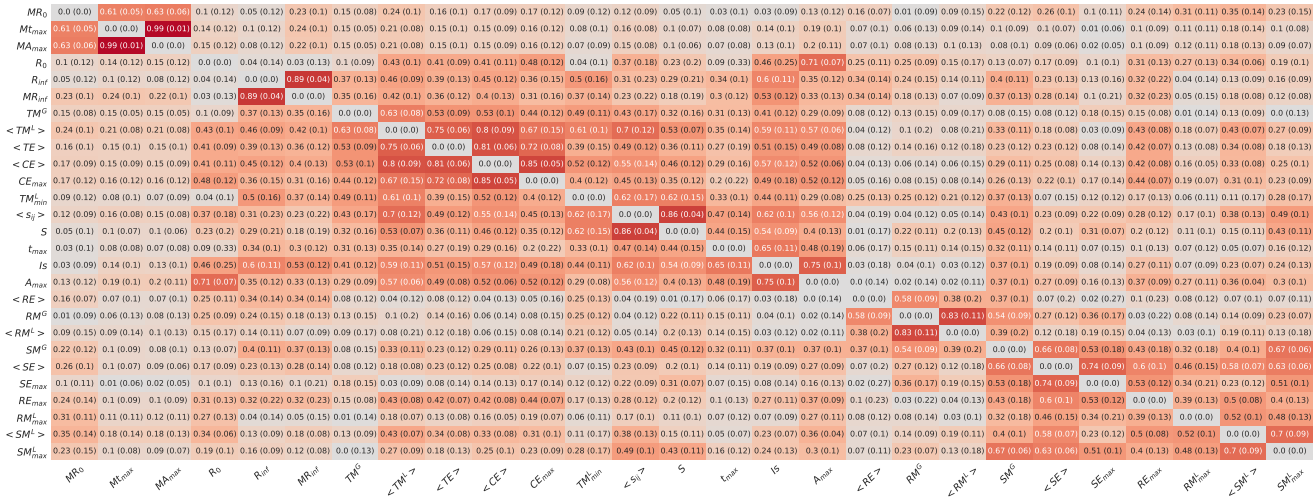

(i) Small communities (5 to 15 species)

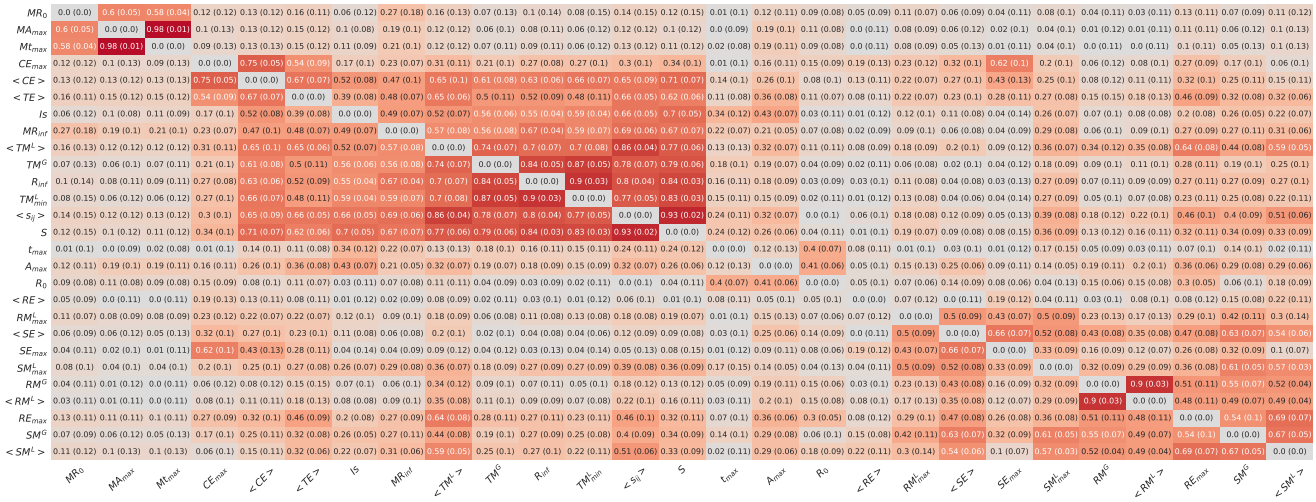

(ii) Medium communities (45 to 55 species)

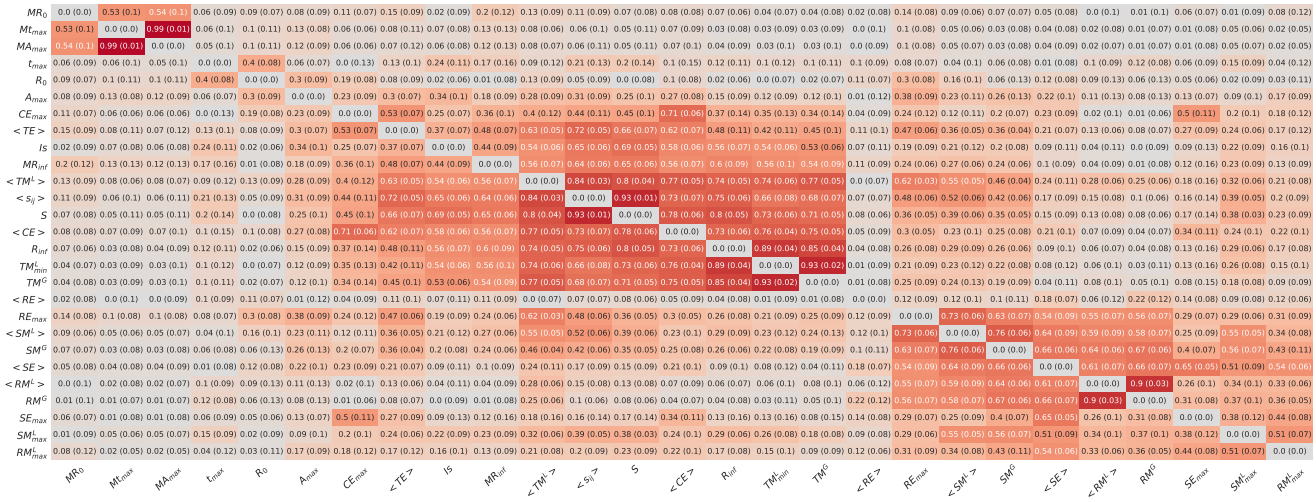

(iii) Large communities (85 to 95 species)

Fig. S5. Correlation matrix between all stability metrics. Each matrix element represents the average pairwise correlation over all the community sizes, as well as the standard deviation in brackets.

6. Analysis of explained variance

After finding the three different stability groups that can be identified with different stability components (or 'dimensions') one question that naturally arises is if is possible to simplify the assessment of stability by choosing only one metric from each group, and if so, how much of the original total variability would be retained.

A first important point to mention is that we measure a number of stability metrics on ecological networks, but we don't have an independent measure of 'total stability'. There is indeed no way of measuring the overall stability of a system outside the information provided by all the different stability metrics. We therefore estimate total stability as the combination of (or information provided by) all the metrics measured. Because of the high correlations between our metrics, we focus on the variance-covariance matrix rather than performing a PCA (which is nonetheless related). The underlying idea is that this matrix quantifies the overall variability of all metrics taken together. Indeed, if there is no correlation among metrics, each of them contains different information and a metric's contribution to the overall variance of 'total stability' can be estimated by the proportion of that metric's variance, i.e. the variance of that metric divided by total variance (which is the sum of the variances of all metrics). However, when metrics are correlated, they contain partially redundant information. In this case, using a single metric 'explains' more of the overall variance than the variance of the metric itself because it also provides information on the other metrics it is correlated with. Note that in this analysis we use the term 'explain' in a loose sense, because it has no real explanatory value as we don't have an independent measure of total stability. It rather quantifies the contribution of a metric to the variability of the total stability. To estimate the proportion of the original variance that is explained by a single metric taking into account its covariance with other metrics, we use the following expression (13):

$$EV_i = \frac{\sum_m C_{im}^2 / C_{ii}}{Tr(\hat{C})} \quad [1]$$

where EV_i is the proportion of explained variance of a given metric i, $\hat{C}$ is the covariance matrix of all the stability metrics, C_{im} are the elements of matrix $\hat{C}$, and m are all the different metrics initially considered. Note that in the case of independent metrics (i.e. having zero covariance with other metrics), we recover the expression $EV_i = C_{ii}/Tr(\hat{C})$, where each metric only accounts for the proportion of variability it contributes to the total.

To calculate the explained variance EV_i from Eq. (1), we first obtain the covariance matrices of the stability metric values for the three different ranges of community sizes analyzed in the here (small, medium and large), as follows. For each community size, ranging from 5 to 100 species, we sample 100 trophic communities of each size, mean-normalise each metric across all communities (which preserves the original variability of each metric but puts all of them in a similar scale), and compute the covariances. We assemble covariance matrices for different classes of community sizes, namely small (5-15 species), medium (45-55 species), and large (85-95 species), by considering the average value of the covariance within these size ranges.
Once the covariance matrices are obtained for the three network sizes, we rank the metrics according to the estimated 'explained' variance (see Fig. S6 below; the total heights of the bars represent, for each metric, its 'explained' variance taking covariances into account using Eq.(1)). In addition, we also plot (in red) the proportion of variance of each metric (i.e. its variance divided by the sum of all variances, without taking covariances into account, or as if the metrics were uncorrelated). Lastly, each metric is colored according to the metric group it belongs to (see Fig. 2 in the main text).

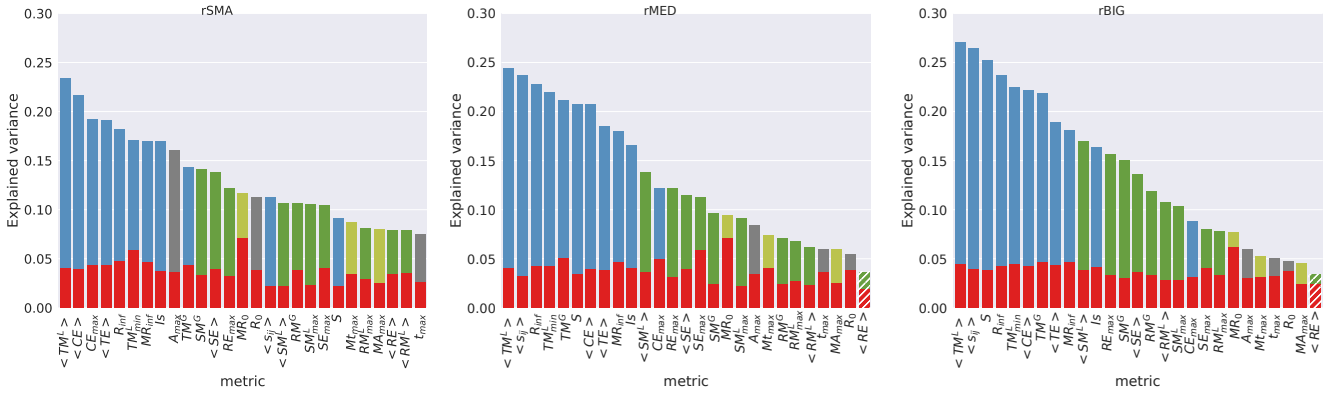

(i) Small communities (5 to 15 species)

(ii) Medium communities (45 to 55 species)

(iii) Large communities (85 to 95 species)

Fig. S6. *'Explained' variance as measured by Eq. (1) for each of the 27 metrics for the three different community sizes analyzed. For each metric, 'explained' variance is subdivided in a variance part in red and a covariance part, whose color depends on the stability group each metric belongs to. As in the main text, blue represents metrics from the 'Distance to threshold' group, green the metrics from the 'Sensitivities to press' group, and light green the metrics from the 'Early response to pulse' group. In gray are the three metrics that were not clearly assigned to any of the groups. The metric in the stripped pattern is the outlier that was not included in the same group by the modularity algorithm and hierarchical clustering.*

The analysis reveals that not all metrics are equally variable, and that, when not considering covariances, each of them accounts for a relatively small proportion of the overall variance (max 8%; red bars in Fig. S6). When taking the covariances into account, these proportions change considerably for all metrics. We can thereby identify the metrics that explain the most variance overall, and also those that explain the most variance in a given group.

Following this, we would like to have an idea of how much variability is explained if we only keep a single metric from each group, meaning three metrics overall. Assuming that the groups are largely independent from each other (given that the average inter-group correlation is ∼0.13) we can estimate the explained variance of such a subset of three metrics by the sum of their explained variance, as if they where independent of each other. To do that, first we remove from the analyses the metrics that were not clearly placed into any group: the three metrics in grey in Fig. S6 (and in Fig. 2 in the main text and Fig. S3ii and S3iii) as well as the measure of average change in total biomass before and after a random extinction ($< RE >$), represented with a stripped pattern in Fig. S6 (and in Fig. 2 in the main text and Fig. S3ii and S3iii). We end up with a total of 23 metrics. Then, we recalculate the proportion of the total original variance (of the remaining 23 metrics) explained by each metric as in Eq. (1) and obtain the explained variance by different subsets of three 'independent metrics' (one from each of the three groups) by adding their proportions of explained variance.

Choosing specifically the best-of-each group metric based on explained variance (i.e. the average species tolerance to increased mortality ($< TM^L >$), the average sensitivity of species biomass to a global mortality increase ($< SM^G >$), and the median reactivity (MR_0) in small networks; the average species tolerance to increased mortality ($< TM^L >$), the average sensitivity of species biomass to a local mortality increase ($< SM^L >$) and the median reactivity (MR_0) in medium and large networks), we find that these 3 metrics account for 53%, 52% and 59% of the original total variance in small, medium and large communities. Conversely, the three worst-of-each group metrics explain 27%, 27%, and 24% of the variance. For comparison, we measure the average explained variance by three randomly selected metrics (with the constraint to have one metric from each group) and obtained 41%, 42%, and 44% (with a standard deviation of 5%) of explained variance in small, medium and large communities. When choosing the most correlated metric from each stability group (i.e median maximum amplification (MA_{max}), average species tolerance to increased mortality ($< TM^L >$), and sensitivity of species biomass to a global mortality increase (SM^G) in small networks; median maximum amplification (MA_{max}), Sensitivity metric based on the inverse Jacobian (S) and sensitivity of species biomass to a global mortality increase (SM^G) in medium networks; median maximum amplification (MA_{max}), Sensitivity metric based on the inverse Jacobian (S), and average sensitivity of species biomass to random extinctions ($< SE >$) on large networks) we find that these 3 metrics account for 48%, 41% and 49% of the total variability respectively in small, medium and large networks. While the most correlated metrics are not the ones that explain more variance in all groups, they close or above the average value explained when the metrics are chosen randomly.

In conclusion, this analysis provides a first answer at how well one would retain the original variability if one wanted to choose a small number of metrics to measure, while using one from each stability 'component'. However, the choice of the metrics to be measured will always depend on the system studied and the practicality of how metrics can be measured. This preliminary analysis can be of use to make informed choices at this respect.

7. Volume of covariance ellipsoid and stability dimensions

We perform an analysis to estimate to what extent the metrics of different groups measure different 'dimensions' of stability. In other terms, how relevant is it to select the three metrics from the three different groups? Following the work of Donohue *et al.* (11), we estimate the volume of the covariance ellipsoid associated to sets of three different metrics. The idea behind this analysis is that the volume of the covariance ellipsoid is a proxy for the dimensionality of stability. If the covariance ellipsoid shape is close to a sphere, the three metrics will be considered to be independent from each other and reflect different dimensions of stability. On the other hand, if the covariance ellipsoid shape is closer to a cigar, it has a smaller volume than in the first case and this means that the three metrics considered reflect a smaller number of stability dimensions.

To calculate the volume of the covariance ellipsoids, we first obtain the covariance matrices of the metrics (based on their rank) for the three different network sizes: small (5 to 10 species), medium-sized (45 to 55 species) and large communities (85 to 95 species) as follows. For each community size, ranging from 5 to 100 species, we sample 100 trophic communities of each size, and compute the pairwise covariances among all stability metrics (based on their rank). We build the rank covariance matrices for the three different community sizes by considering the average value of pairwise covariance within these size ranges.

Once we have the covariance matrices, we randomly select three stability metrics out of the 23 stability metrics that were clearly assigned to a group in two different ways: i) by randomly selecting three metrics from the same group (we did this for the three groups), and ii) by randomly selecting one metric from each group. Once the sets of three metrics are determined, we extract the corresponding rows and columns of the covariance matrix to generate a 'reduced' version of the covariance matrix with only 3 metrics. Finally, we diagonalize the 'reduced' covariance matrices to obtain the eigenvalues and calculate the ellipsoid volume (V) using the formula:

$$V = \frac{\pi^{m/2}}{\Gamma(\frac{m}{2}+1)} \prod_{i=1}^{m} (\sqrt{\lambda_i}) \qquad [2]$$

where λ_i is the i-th eigenvalue of the covariance matrix, and m is the number of dimensions considered, three in our case (14).

We repeat this procedure 2000 times to obtain the average volume of the covariance ellipsoid associated with three metrics coming either from the same or from different groups. The results show that, although choosing 3 metrics within the same group can in some case still lead to a relatively large volume (Fig. S7 below), it is only when the three metrics are selected from different groups that the highest volume is obtained, meaning that the better the dimensionality of stability is reflected. This is especially true in large networks (Fig. S7iii), where the volume obtained with metrics from different groups reaches a proportion between 0.9 to 0.96 of the maximum attainable volume (where 1 means a complete independence of the three dimensions) whereas selecting the most different metrics within any of the other groups (i.e. those that maximize the ellipsoid volume) only achieves at most proportions of 0.13, 0.64 or 0.73 for each of the three groups respectively.

This result is not surprising as the objective of the analysis performed was precisely to identify such the groups. However, this analysis, using a slightly different approach, is a nice confirmation that the groups identified reflect different dimensions, and that selecting metrics in each of them improves the dimensionality of stability represented compared to selecting the same number of metrics in a given group.

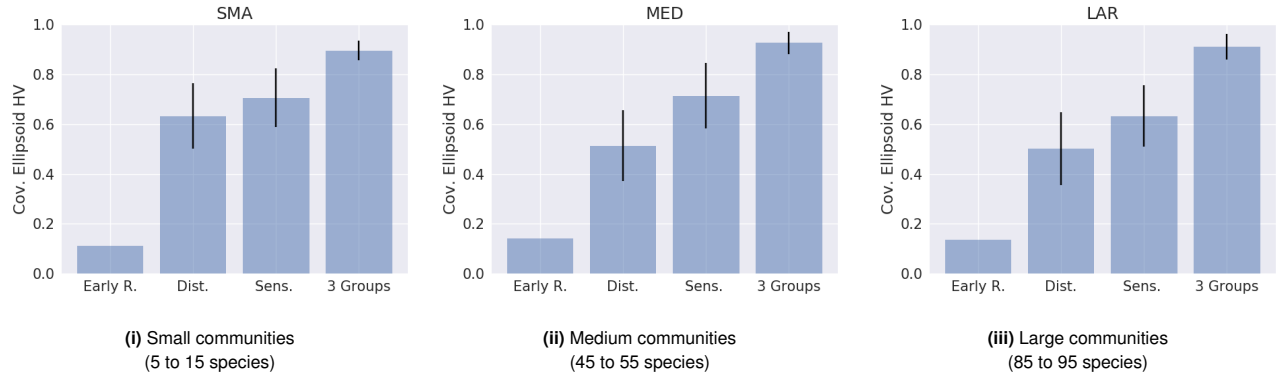

Fig. S7. *Volume of the covariance ellipsoid as quantified by Eq.(2) for the three different network sizes studied. For each richness level, we measure the volume of the covariance ellipsoid defined by three randomly picked stability metrics. The height of the first three bars on each figure represents the volume obtained when the three metrics are taken within the same group ('Early response to pulse', 'Distance to threshold' and 'Sensitivities to press' respectively); the fourth bar represents the volume obtained when the three metrics are selected from the three different groups. The whiskers represent the standard deviation of the volume. All values were normalized to the maximum possible value for an ellipsoid in three dimensions, which happens when the three metrics are perfectly independent ($V = 0.8061$))*

Supporting Information for Methods

8. Dynamic Food-Web Model

We use an allometric-scaling dynamic food web-model to simulate the biomass of each species (15, 16). These models have been used extensively to explore the dynamics and stability of complex ecological networks (15, 17). The trophic community consists of plants (primary producers, at the base of the network), and consumers (animals that eat plants and/or other consumers). The number of species N and connectance c (density of trophic interactions) are initial parameters. The structure of the food-web (who eats whom) is initially determined by the niche model (18). We map dynamical consumer-resource equations to that food-web skeleton to model the biomass of each species. The change in species i's biomass density B_i is described by an ordinary differential equation of the general form (19):

$$\frac{dB_i}{dt} = r_i G_i B_i + B_i \sum_{j \in prey} e_{0j} F_{ij} - \sum_{k \in pred} B_k F_{ki} - x_i B_i - d_i B_i \quad [3]$$

where the first term describes plant growth; the second term describes the biomass gained by consumption of other species j; the third term describes mortality due to predation, summed over all consumers k of species i; the fourth term represents the metabolic demands of species i; the last term is natural mortality of species i. More precisely:

- r_i is the intrinsic growth rate of primary producers ; r_i is 1 for primary producers and null for other species.
- G_i is the growth term described in equation 4 below.
- e_{0j} is the conversion efficiency which determines how much biomass eaten of resource j is converted into biomass of consumer i. Is set to 0.45 if the resource j is a plant and to 0.85 otherwise.
- F_{ij} is the functional response, i.e. the rate at which consumer i feeds on resource j (see equation 5 below).
- x_i is the metabolic demand of species i. If i is a plant, $x_i = 0.138 m^{0.25}$. If i is not a plant $x_i = 0.314 m_i^{0.25}$.
- d_i is the natural mortality rate. It is assumed to be $d_0 x_{species} {m_i}^{0.25}$ with $d_0 = 0.1$ and $x_{species} = 0.138$ if i is a plant and 0.314 otherwise.

A. Plant growth. We assume a logistic growth for basal species:

$$G_i = (1 - \frac{B_i}{K_i}) \quad [4]$$

with K_i being the carrying capacity of the environment for species i. We fix this value to 1.

B. Functional response. We use a multi-prey Holling-type functional response. The feeding rate of species i on species j is expressed as:

$$F_{ij} = \frac{w_i a_{ij} B_j^{1+q}}{m_i (1 + w_i \sum_{k \in prey} a_{ik} h_{ik} B_k^{1+q})} \quad [5]$$

where:

- w_i is the relative consumption rate of predator i on its prey, which accounts for the fact that a consumer has to split its consumption between its different resources.
- The attack rate is $a_{ij} B_j^q$, where a_{ij} is the capture coefficient. If i and j are not plants $a_{ij} = a_0 {m_i}^{\alpha_i} {m_j}^{\alpha_j}$ with $a_0 = 50$. If the resource is a plant then the capture coefficient is $a_{ij} = a_{0plant} {m_i}^{\alpha_i}$, and $a_{0plant} = 10$. The exponents α_i and α_j were sampled from normal distributions with mean $\mu_{\alpha_i} = 0.7$ and $\mu_{\alpha_j} = 0.4$ and s.d of $\sigma_\alpha = 0.1$, the average values as presented in (20).
- $1 + q$ is the Hill-exponent, where the Hill-coefficient q varies the functional response gradually from a type II ($q = 0$) to a type III ($q = 1$) (21). Trough the main text results we use $q = 0.3$.
- h_{ij} is the handling time in $\frac{[time]}{[mass]}$, with $h_{ij} = h_0 {m_i}^{H_i} {m_j}^{H_j}$. The exponents where sampled from normal distributions with mean $\mu_{H_i} = -0.6$ and $\mu_{H_j} = -0.5$ and s.d $\sigma_H = 0.1$, the average values as presented in (20).

9. Detailed simulation procedure

We simulate realistic trophic communities using an allometric-scaling dynamical food-web model (16, 22), explained in the previous section, where all the species biological rates scale with the mass of the species, which in turn, scales with the trophic level. These kinds of models have been widely used to study the stability of trophic communities with high success and provide a more accurate description than previous more simplistic ones (17, 22, 23). We generate the backbone of the networks with an initial species richness ranging from 5 to 115 species and a fixed connectance (c= 0.15). The feeding interactions among the species are established by using the 'niche model' (18). Once this skeleton has been assembled, the dynamical equations are mapped on it, and the community evolves until it reaches a steady state. With this framework we obtain a dynamical viable trophic network where the interactions are a result of both dynamical and structural constraints. The detailed process is as follows:

- Generate a trophic network skeleton with N species and NL links, according to the niche model. The initial number of species N varies from 5 to 115 and the probability of a trophic interaction (i.e. the probability that i eats j and that A_{ij}=1 in the adjacency matrix) is $p = NL/N^2 = 0.15$.

- Obtain the trophic level of each species in the community, L_i. The L_i of all plants is set to 1, while the trophic level of consumers is calculated as the average of the trophic level of their prey plus one. In the cases where the structure of the network has inconsistencies and the trophic levels cannot be calculated (e.g. lack of basal species for example, or a closed and isolated loop), the network is discarded and a new one is generated.

- Once the trophic levels are determined, we set the masses of the species to $m_i = Z^{(L_i-1)}$, where Z is the ratio between predator and prey body mass. The mass of all basal species is set to 1. We use a value of Z equal to 1.5.

- Calculate all biological rates that take part in the functional response (r_i, x_i, d_i, a_{ij}, h_{ij}) as described in the model description (see previous section).

- Apply the dynamical equations. In some cases during the dynamical evolution of the system, some of the species will go extinct because their interactions are not energetically viable. A species will be considered extinct if at a given time its biomass density falls bellow the extinction threshold, $extinctthres_i = 1E^{-6} * m_i$. In this case its biomass is set to 0 and the interactions of this species are deleted from the interaction matrix A.

- Keep running the simulations until either a steady state is reached, or until the maximum amount of time for the simulation is reached ($T_{SAFE} = 1000000$). The steady state is reached if the biomass change of all individual species, $\Delta Log(b_i)$, is less than $\sigma_b = 0.0005$ for a given temporal window (Δt). If such a state is reached, we have a dynamically viable and realistic trophic community, that we proceed to study. If T_{SAFE} is reached before the system has arrived to a steady state, the community is discarded and we start again by generating a new trophic network and following all the subsequent steps. In this way we make sure that we will only study systems whose equilibrium is "static" without oscillations in the populations.

- Once a viable dynamic trophic community has been obtained and before we proceed to study it, we search for isolated plants and delete them by setting their biomass density to 0. These isolated species do not play a role in the community since they do not take part in any interaction, but they can artificially increase the number of species. We only keep networks with at least 90% of surviving species to ensure that the interaction strengths are not too reduced because of absent species.

The code for running the simulations is available upon request.

10. Stability Metrics Definitions

Responses to pulse perturbations.

Reactivity (R_0): Maximal instantaneous rate at which initial perturbations can be amplified. It measures the initial response to the perturbation. It is defined as:

$$R_0 = -\tfrac{1}{2}\lambda_{dom}(C_{sim}) \quad [6]$$

were C is the Community matrix, or Jacobian, obtained by calculating the derivatives of the dynamical equations and substituting the biomasses of species at the fixed point (i.e. once all species have reached the steady state). C_{sim} is the symmetric matrix of the Jacobian, defined as $C + C^T = C_{sim}$. If $R_0 < 0$, the perturbation first increases before it decays and the system is said to be *reactive*. This is a measure of the initial behaviour of the system response (12).

Maximal amplification (A_{max}): Factor by which the perturbation that grows the largest is amplified. It is quantified as the maximum value of the amplification envelope $A(t)$. This function, that describes the time evolution of the perturbation, can be computed as the matrix norm of e^{Ct} (12).

$$A(t) = max_{x_0 \neq 0} \frac{\parallel e^{Ct} x_0 \parallel}{\parallel x_0 \parallel} \quad [7]$$

We use the function "expmat" in the armadillo library in C++ to obtain the amplification envelop of the Jacobian matrix, and determine the maximum amplitude as the maximum value of A(t)

$$A_{max} = max_{t \geq 0} A(t) \quad [8]$$

This is a measure of the transient regime of the system (neither initial nor asymptotic).

Time to maximal amplification (t_{max}): Time at which the system reaches the maximal amplification. Obtained as as presented in (12).

$$A(t_{max}) = A_{max} \quad [9]$$

Resilience (R_{inf}): Asymptotic return rate to the reference state after a pulse perturbation. In theoretical studies, the return time is often approximated as the reciprocal of asymptotic resilience. In this approach, initiated by Pimm & Lawton (24, 25), asymptotic resilience is quantified as the leading eigenvalue of the Jacobian, also referred to as the 'community matrix',

$$R_{inf} = -\Re(\lambda_{dom}(C)) \quad [10]$$

Median values for the whole community: As showed in previous analytical works studying pulse perturbations, all the metrics presented so far are mostly defined by individual species, and hence we can see them as "extremal metrics". In order to obtain metrics that are more representative of the whole community, we apply the formulation presented in (26) to calculate the median values of all those metrics over perturbation directions for the whole community. Following the approach in (26), we assume that the perturbation affecting the biomass of a given species is proportional to its equilibrium biomass. As the authors show, it is enough to know the Jacobian matrix, A and the correlation matrix of the perturbations, C, to obtain these metrics. For a detailed information on how to compute C we refer the reader to the original paper.

-Median reactivity (MR_0): Median rate of displacement from equilibrium immediately after a pulse perturbation. It is computed as

$$MR_0 \approx \frac{Tr\,(CA)}{TrC} \quad [11]$$

-Median maximal amplificaton (MA_{max}): Factor by which the median displacement is amplified. That is, the maximum value of the median displacement, calculated as

$$M\left(x^2\right) \approx Tr\left(Ce^{A^T t} e^{At}\right) \quad [12]$$

-Median time to maximal amplificaton (Mt_{max}): Time at which MA_{max} is reached.

-Median Resilience (MR_{inf}): The median return rate averaged over time, is calculated as

$$MR_{inf} \approx -\frac{ln\left(Tr(Ce^{A^T t} e^{At})\right)}{2t} \quad [13]$$

where we consider that the asymptotic limit is reached if the displacement is below a threshold of 0.005.

Responses to continuous shocks (environmental stochasticity).

Intrinsic stochastic invariability (I_S) : Stationary response of the linearized system to stochastic perturbations of zero-mean and persisting through time (white noise). I_S is inversely proportional to the variance of the maximal response to white-noise perturbations. It can be computed as:

$$Is = \frac{1}{2} \parallel -\hat{C}^{-1} \parallel^{-1} \quad [14]$$

where $\hat{C} = C \otimes 1 + 1 \otimes C$, and $\parallel . \parallel$ is the spectral norm of the matrix (26). We also used the armadillo library in C++ for these calculations.

Responses to press perturbations.

Sensitivity (S, $< s_{ij} >$): Following the theoretical study of press perturbations from the sensitivity matrix as presented in (8, 27), we define a metric to quantify this response. The metric we propose to quantify the community response is the total displacement experience by the the community biomass, that is, the sum of the absolute changes in populations species biomasses computed as:

$$S = \sum_i |\sum_j S_{ij}| \quad [15]$$

where S stands for the Sensitivity matrix, i.e. the inverse of the community matrix and is obtained as $S = -C^{-1}$. To obtain the metric at the species' scale we used the approach of Carpenter et al. (28) and measured the average strength of the elements of the sensitivity matrix

$$< s_{ij} >= \sum_i \sum_j |s_{ij}|/(N^2) \quad [16]$$

When using these methods one typically assumes that pre- and post-perturbed systems are close to fixed-point steady states and that perturbations are sufficiently small.

Tolerance to increased mortality (TM^G): Maximum magnitude of disturbances that the community can tolerate before any species goes extinct. This is a metric of "structural stability" (5, 29) since it gives information on the amount of change allowed in the parameters before the system changes dramatically. We implement an empirical approach and follow the method described in (6) (although the authors name this measure *resistance*, we are going to use the term *tolerance* here to avoid confusion with the more historical definition of resistance, which refers to a net change in a system's property (e.g. total biomass) before and after a perturbation). A system with a higher tolerance can withstand larger increases in mortality rates before any extinction occurs.
To measure this behaviour, we subjected each trophic community to simulated press disturbances to quantify their tolerance. For all species in the network, the mortality rate is simultaneously increased (global 'attack') as $d'_i = d_i + \Delta_d * d_i$, with $\Delta_d = 0.1$ until some species goes extinct (the attacked species or any other). Following (6) the tolerance of the whole community is considered to be that of the less tolerant species

$$TM^G = \frac{min(d'_i) - d_i}{d_i} \quad [17]$$

To study the response to individual species changes (local 'attack'), we also increased the death rate of the species with the same strength as above but one by one. In this case the tolerance of each species is defined as the minimum increase in its death rate that can be sustained before any species of the community goes extinct. We recorded the average tolerance of all species in the community $< TM^L >$ and that of the least tolerant species TM^L_{min}. This measure is also related to that of Effective Population Size (EEP) defined to study the functional extinctions (30).

Tolerance to extinctions (TE): In order to account for the tolerance to extinctions of random species, we use 'Robustness' as defined in (31) and quantify the fraction of species that had to be removed from the community in order to result in a total loss of 50% of the species (i.e. primary species removals plus secondary extinctions). The procedure is as follows: we perform the extinction of a random species and let the system evolve until a fixed point is reached and secondary extinctions have taken place. Then we continue to erase another species in the same fashion, in a random order, until at least half of the original community is destroyed. The number of primary random extinctions we need to perform before attaining that point is what we named the tolerance to extinctions. As this metric depends on the order in which the species are selected to be primarily erased, we perform 100 random sequences of extinctions and take the average tolerance to obtain $< TE >$.

Resistance metrics to increased mortality:

Resistance metrics are a general way to measure the amount of change in the state of a system before and after a sustained perturbation. To measure the resistance of communities to an increased mortality, we perform simulations where all species death rates are simultanesouly increased by 10% and wait for the community to arrive at the new equilibrium (in some cases extinctions occur). We measure the differences between the initial and the final state for different variables.

Resistance of total biomass to increase in mortality (RM): Following a similar approach as Ives (32), we compute the total change in community biomass before and after the mortality increase as the total change in biomass divided by the change in the stressor. In our case the change in the stressor is constant (10% increase in mortality), so resistance is measured as

$$RM^G = \frac{-|B_0 - B'|}{B_0} \quad [18]$$

where B_0 is the total biomass of the original community and B' the total biomass of the community in the post-perturbed state. Unlike in the reference (32) we have, we divide by B_0 to obtain relative resistances, since we will be comparing many different communities with different total biomasses. The absolute value is to account for the fact that either a net gain or loss of total biomass is considered as a deviation from the original reference state. With this metric, the larger the deviation (positive or negative), the less resistant the community is.

We also measured the average total biomass resistance when only one of the species is perturbed (as done in (32)), by increasing the mortality of each species one by one and measuring the resistance to mortality in each case as described above. The average value is recorded as $< RM^L >$ and the maximum displacement as RM^L_{max}.

Sensitivity of species' biomass to increase in mortality (SM): We compute the total change in biomass in front of a global mortality increase as the norm of the difference in species' biomass

$$SM^G = \frac{-\ell_1(B_0 - B')}{B_0} \quad [19]$$

where ℓ_1 stand for the L1-norm of the vector of differences in biomass. This quantity measures the total amount of change the populations have suffered, even if it is not apparent in the total biomass change, due to compensatory effects in the dynamics. As in the case above we also measure the average and the maximum sensitivity of populations when only one species is attacked ($< SM^L >$ and SM^L_{max}).

Resistance metrics to species extinctions:

We measure the resistance of the whole community to species extinctions by comparing different variables before and after a species extinction takes place.

Resistance of community composition to random extinctions (CE) : In this case, we measure the cascading extinctions after a random extinction from the species in the community, as done in (33). We compute this by sequentially deleting one species at a time and measuring the number of secondary extinctions produced (i.e. the number of additional species that go extinct as a consequence of that first species deletion). The value ($< CE >$) is the average number of secondary extinctions over all extinction events (i.e. after all species of the community have been driven to extinction, one by one). We also record the maximum number of cascading extinctions as (CE_{max}).

Resistance of total biomass to a random species deletion (RE): We are also interested in knowing how the total aggregated biomass of the community is affected by a species loss, as studied in (33). Following a similar procedure as the one used for the resistance to increased mortality, we measure the resistance of community biomass to a species loss as the total change in community biomass before and after one species extinction (and possible secondary extinctions) has taken place. The value for the community is the average value obtained after each of the species composing the community is erased:

$$< RE >= -\left\langle \frac{|B_0 - B''|}{B_0} \right\rangle \quad [20]$$

where B'' represent the state of the post-perturbed community. We also retained the maximum change in biomass as a result of one species extinction, as RE_{max}. The absolute value in the definition is to account for the fact that either gain or loss in community biomass is a deviation from the original state. The bigger $< RE >$, the further away a community is from the original value of total biomass.

Sensitivity of species' biomass to random species deletions (SE): In a similar fashion as the sensitivity of species' biomass to increased mortality, we compared all the species' biomasses before and after a random extinction, and obtained the average accumulated difference in species' biomasses averaged over all extinction events, -i.e leading each of the species in the community to extinction once-.

$$< SE >= -\left\langle \frac{\ell_1(B0 - B'')}{B_{tot}} \right\rangle \quad [21]$$

We also recorded the maximum total displacement in species biomass as a result of one extinction as SE_{max}.

References

1. Arnoldi JF, Bideault A, Loreau M, Haegeman B (2018) How ecosystems recover from pulse perturbations: A theory of short- to long-term responses. *Journal of Theoretical Biology* 436:79–92.
2. Fortunato S (2010) Community detection in graphs. *Physics Reports* 486(3-5):75–174.
3. Ştefan RM (2014) Cluster type methodologies for grouping data. *Procedia Economics and Finance* 15:357–362.
4. Illingworth V (1991) The penguin dictionary of physics.
5. Rohr RP, Saavedra S, Bascompte J (2014) On the structural stability of mutualistic systems. *Science* 345(6195):1253497–1253497.
6. Wootton KL, Stouffer DB (2016) Species' traits and food-web complexity interactively affect a food web's response to press disturbance. *Ecosphere* 7(11):e01518.
7. Dakos V, Bascompte J (2014) Critical slowing down as early warning for the onset of collapse in mutualistic communities. *Proceedings of the National Academy of Sciences* 111(49):17546–17551.
8. Nakajima H (1992) Sensitivity and stability of flow networks. *Ecological Modelling* 62(1-3):123–133.
9. Arnoldi JF, Haegeman B (2016) Unifying dynamical and structural stability of equilibria. *Proceedings of the Royal Society A: Mathematical, Physical and Engineering Science* 472(2193):20150874.
10. Pennekamp F, et al. (2018) Biodiversity increases and decreases ecosystem stability. *Nature* 563:109–112.
11. Donohue I, et al. (2013) On the dimensionality of ecological stability. *Ecology Letters* 16(4):421–429.
12. Neubert MG, Caswell H (1997) Alternatives to resilience for measuring the responses of ecological systems to perturbations. *Ecology* 78(3):653–665.
13. (year?) Pca - variance of the data explained by a single variable (https://stats.stackexchange.com/questions/52828/variance-of-the-data-explained-by-a-single-variable). Accessed: 30-07-2019.
14. Wilson AJ (2009) Volume of n-dimensional ellipsoid. *Sciencia Acta Xaveriana* 1(1):101–106.
15. Brose U, Williams RJ, Martinez ND (2006) Allometric scaling enhances stability in complex food webs. *Ecology Letters* 9(11):1228–1236.
16. Yodzis P, Innes S (1992) Body Size and Consumer-Resource Dynamics. *The American Naturalist* 139(6):1151–1175.
17. Williams RJ, Martinez ND, Williams RJ, Martinez ND (2004) Stabilization of chaotic and non-permanent food-web dynamics. *Eur. Phys. J. B* pp. 297–303.
18. Williams RJ, Martinez ND (2000) Simple rules yield complex food webs. *Nature* 404(6774):180–183.
19. Kéfi S, Miele V, Wieters EA, Navarrete SA, Berlow EL (2016) How structured is the entangled bank? the surprisingly simple organization of multiplex ecological networks leads to increased persistence and resilience. *PLOS Biology* 14(8):e1002527.
20. Rall BC, et al. (2012) Universal temperature and body-mass scaling of feeding rates. *Philosophical Transactions of the Royal Society B: Biological Sciences* 367(1605):2923–2934.
21. Real LA (1977) The kinetics of functional response. *The American Naturalist* 111(978):289–300.
22. Brose U, et al. (2008) Foraging theory predicts predator-prey energy fluxes. *Journal of Animal Ecology* 77(5):1072–1078.
23. Berlow EL, et al. (2008) Simple prediction of interaction strengths in complex food webs. *Proceedings of the National Academy of Sciences* 106(1):187–191.
24. Pimm SL, Lawton JH (1977) Number of trophic levels in ecological communities. *Nature* 268(5618):329–331.
25. Pimm SL, Lawton JH (1978) On feeding on more than one trophic level. *Nature* 275(5680):542–544.
26. Arnoldi JF, Loreau M, Haegeman B (2016) Resilience, reactivity and variability: A mathematical comparison of ecological stability measures. *Journal of Theoretical Biology* 389:47–59.
27. Bender EA, Case TJ, Gilpin ME (1984) Perturbation experiments in community ecology: Theory and practice. *Ecology* 65(1):1–13.
28. Carpenter SR, et al. (1992) Resilience and resistance of a lake phosphorus cycle before and after food web manipulation. *The American Naturalist* 140(5):781–798.
29. Grilli J, et al. (2017) Feasibility and coexistence of large ecological communities. *Nature Communications* 8.
30. Säterberg T, Sellman S, Ebenman B (2013) High frequency of functional extinctions in ecological networks. *Nature* 499(7459):468–470.
31. Dunne JA, Williams RJ, Martinez ND (2002) Network structure and biodiversity loss in food webs: robustness increases with connectance. *Ecology Letters* 5(4):558–567.
32. Ives AR, Cardinale BJ (2004) Food-web interactions govern the resistance of communities after non-random extinctions. *Nature* 429:174–177.
33. Thébault E, Huber V, Loreau M (2007) Cascading extinctions and ecosystem functioning: contrasting effects of diversity depending on food web structure. *Oikos* 116:163–173.